Indian Journal of Geo Marine Sciences
Vol. 50 (11), November 2021, pp. 890-896

Recursive parameter identification for second-order K-T equations of marine robot in horizontal motion

Y M Zhong[a], C Y Yu*[,a,b,c], C H Liu[a], T M Liu[b], R Wang[a] & L Lian[a,c]

[a]School of Oceanography, Shanghai Jiao Tong University, Shanghai – 200 030, China

[b]Key Laboratory of Marine Environmental Survey Technology and Application, Ministry of Natural Resources, P. R. China

[c]State Key Laboratory of Ocean Engineering, Shanghai Jiao Tong University, Shanghai – 200 240, China

*[E-mail: yucaoyang@sjtu.edu.cn]

Received 31 August 2021; revised 30 November 2021

In this paper, a dedicated recursive least squares algorithm combining forgetting and weighted factors (FW-RLS) is proposed to identify parameters for the second-order K-T equation of marine robot in horizontal motion. First, the Abkowitz model in horizontal motion is converted into an equivalent second-order K-T equation to reduce the number of identification parameters. Second, a dedicated FW-RLS algorithm based on the equivalent second-order K-T equation is proposed. Finally, the superiority of the FW-RLS algorithm is verified by comparative numerical simulations, which show the FW-RLS algorithm has the online identification capability, higher identification accuracy, and faster convergence rate compared with the traditional batch least squares method.

[**Keywords**: K-T equation, Least squares method, Marine robot, Parameter identification]

Introduction

With the development of communication technology and artificial intelligence, marine robots have been increasingly used in civil, scientific, and military fields[1-4]. At present, the motion control of the marine robot, especially its horizontal motion control, is essential for accurate control[5-8]. It is well known that establishing a precise motion model of a marine robot is the basis for achieving the accuracy of motion control[9-10]. However, when the marine robot operates in a complex maritime environment, its dynamics will be influenced by hull shape and external environmental factors such as sea wind, waves, and current flow. Therefore, the motion model of the marine robot is complicated[11]. For this reason, how to obtain accurate motion models of marine robots deserves further research.

Currently, the following methods are available to obtain the ship's motion model parameters: self-propelled model test[12], direct numerical simulation methods based on computational fluid dynamics (CFD)[13], and parameter identification (PI)[14-16]. Among them, the self-propelled model test requires special test equipment and a large amount of experimental data. Apart from that, the CFD method is used to obtain the ship's motion parameters in a purely numerical way by first solving the equations of fluid motion and rigid body motion jointly and then numerically simulating the ship's maneuvering motion in a time-stepping method. However, the CFD method is time-consuming. Besides, the PI is a method of considering the ship motion as a dynamic response system, and the system inputs (rudder angle, etc.) and outputs (speed, angular velocity, etc.) are obtained by maneuverability experiments[17]. Based on the above input and output data, the coefficients in the mathematical motion model are accessed using the system identification algorithm. This approach has powerful capabilities in hydrodynamic coefficient prediction and provides a powerful tool for ship maneuvering motion dynamics modeling[18-19].

Traditionally, the commonly used identification techniques in marine engineering include the extended Kalman filter[20], support vector machine[15-18], least squares (LS) [21,22], and so on. In particular, the LS algorithm has the advantages of simplicity and robustness, which is the most widely used identification method[23]. For instance, the weighted least squares method is proposed to speed up the convergence of the identification algorithm[24]. However, when data length is large in the traditional LS, it causes data saturation, making the algorithm

lose the ability to correct. Therefore, the LS with forgetting factor is proposed to overcome data saturation[25,26]. It is expected that the algorithm performance will be further enhanced if both the forgetting factor and the weighted factor are integrated into the LS algorithm. To the best of our knowledge, the recursive least squares algorithm combining forgetting and weighted factors (FW-RLS) has not been applied to the identification of motion parameters of marine robots, so it is worthy of an in-depth study.

In this paper, a dedicated FW-RLS is proposed to implement the parameter identification for the marine robot's K-T equation in horizontal motion, and numerical simulations are presented to demonstrate the superiority of the algorithm. The highlights of this paper are as follows: 1) A second-order K-T equation that contains only four parameters is transformed from the Abkowitz model with many parameters. Then it is utilized for parameter identification of marine robot's maneuvering equation to obtain the heading hydrodynamic characteristics with fewer parameters to be identified; and 2) A dedicated FW-RLS algorithm is proposed to identify the inherent parameters of the marine robot's K-T equation in horizontal motion, which has faster convergence speed, slight overshoot, high identification accuracy, and strong predictive capability.

Materials and Methods

Maneuvering model

For a better description of the motion of marine robot, the Abkowitz model will be used as the basis to construct its maneuvering equation in horizontal motion. The Abkowitz model views the vessel as a whole part, and the forces acting on the vessel as a function of the motion state variables and control variables and expands them in the Taylor series form, as follows:

$$\begin{cases}(m-X_{\dot u})\dot u = f_1(u,v,r,\delta)\\ (m-Y_{\dot v})\dot v + (mx_G - Y_{\dot r})\dot r = f_2(u,v,r,\delta)\\ (mx_G - N_{\dot v})\dot v + (I_z - N_{\dot r})\dot r = f_3(u,v,r,\delta)\end{cases} \quad \dots (1)$$

where, m is the marine robot's mass; x_G is the vertical coordinate of marine robot's center of gravity; u,v,r denote the surge speed, sway speed, and yaw angular velocity, respectively; X_*, Y_*, N_* are the fluid accelerations; f_1, f_2, f_3 are nonlinear functions of the velocity (angular velocity) and rudder angle.

$$f_1 = X_{u|u|}u|u| + X_{vr}vr + X_{rr}r^2 + X_{prop} \quad \dots (2)$$

$$f_2 = Y_{v|v|}v|v| + Y_{r|r|}r|r| + (Y_{ur}u - mx_G u)r + Y_{uv}uv + Y_{uu\delta}u^2\delta \quad \dots (3)$$

$$f_3 = N_{v|v|}v|v| + N_{r|r|}r|r| + (N_{ur}u - mx_G u)r + N_{uv}uv + N_{uu\delta}u^2\delta \quad \dots (4)$$

Remark 1: The above model is from the Remote Environmental Monitoring UnitS (REMUS) model[27]. The REMUS was developed by the Woods Hole Oceanographic Institution, and is a small autonomous underwater vehicle that was designed to work in near-shore waters.

From equations (1)-(4), it can be seen that the Abkowitz model contains nonlinear terms, which cause difficulties in parameter identification. Therefore, ignoring the nonlinear terms, the Abkowitz model is transformed into a horizontal second-order KT model by combining the second and third equations in (1) and is shown below:

$$\ddot r + T_1\dot r + T_2 r = K\delta + T_3\dot\delta \quad \dots (5)$$

where, T_1, T_2, K and T_3 are the maneuvering indices, which are expressed as:

$$\begin{cases} T_1 = \dfrac{N_{uv}u(mx_G - Y_{\dot r}) - Y_{uv}u(I_z - N_{\dot r})}{(m-Y_{\dot v})(I_z - N_{\dot r}) - (mx_G - Y_{\dot r})(mx_G - N_{\dot v})}\\ T_2 = \dfrac{[N_{uv}u(m-Y_{\dot v}) - Y_{uv}u(mx_G - N_{\dot v})]\times[(N_{ur}u - mx_G u)(mx_G - Y_{\dot r}) - (Y_{ur}u - mx_G u)(I_z - N_{\dot r})]}{(m-Y_{\dot v})(I_z - N_{\dot r}) - (mx_G - Y_{\dot r})(mx_G - N_{\dot v})}\\ \quad - \dfrac{[(N_{ur}u - mx_G u)(m-Y_{\dot v}) - (Y_{ur}u - mx_G u)(mx_G - N_{\dot v})]\times[N_{uv}u(mx_G - Y_{\dot r}) - Y_{uv}u(I_z - N_{\dot r})]}{(m-Y_{\dot v})(I_z - N_{\dot r}) - (mx_G - Y_{\dot r})(mx_G - N_{\dot v})}\\ K = \dfrac{[N_{uu\delta}u^2(m-Y_{\dot v}) - Y_{uu\delta}u^2(mx_G - N_{\dot v})]\times[N_{uv}u(mx_G - Y_{\dot r}) - Y_{uv}u(I_z - N_{\dot r})]}{(m-Y_{\dot v})(I_z - N_{\dot r}) - (mx_G - Y_{\dot r})(mx_G - N_{\dot v})}\\ \quad - \dfrac{[N_{uv}u(m-Y_{\dot v}) - Y_{uv}u(mx_G - N_{\dot v})]\times[N_{uu\delta}u^2(mx_G - Y_{\dot r}) - Y_{uu\delta}u^2(I_z - N_{\dot r})]}{(m-Y_{\dot v})(I_z - N_{\dot r}) - (mx_G - Y_{\dot r})(mx_G - N_{\dot v})}\\ T_3 = \dfrac{N_{uu\delta}u^2(m-Y_{\dot v}) - Y_{uu\delta}(mx_G - N_{\dot v})}{(m-Y_{\dot v})(I_z - N_{\dot r}) - (mx_G - Y_{\dot r})(mx_G - N_{\dot v})}\end{cases} \quad \dots (6)$$

For further parameter identification, the variables in equation (5) are treated using the differentiation method, namely:

$$r(k) = \frac{\psi(k) - \psi(k-1)}{h} = \frac{y(k)}{h} \quad \dots (7)$$

where, h is the time interval between two sample points; $y(k)$ is the increment of the yaw angle at moment k.

Therefore, from equations (5) and (7), it is obtained that:

$$y(k) - 2y(k-1) + y(k-2) = -h^2T_2y(k) - hT_1[y(k) - y(k-1)] + h^3K\delta(k) + h^2T_3[\delta(k) - \delta(k-1)] \quad \dots (8)$$

Equation (8) is rewritten in matrix form and can be expressed as $Y(k) = \boldsymbol{H}^T(k)\boldsymbol{q}$, where

$$\boldsymbol{H}(k) = [-h^2y(k) \quad -h(y(k) - y(k-1)) \quad h^3\delta(k) \quad h^2(\delta(k) - \delta(k-1))]^T \quad \dots (9)$$

$$\boldsymbol{\theta}=[T_2 \quad T_1 \quad K \quad T_3]^T \qquad \ldots (10)$$

$$Y(k)=y(k)-2y(k-1)+y(k-2) \qquad \ldots (11)$$

Dedicated FW-RLS algorithm

The core of the FW-RLS algorithm is based on the traditional batch least square (BLS) algorithm, so the following criterion function for the BLS algorithm is constructed as:

$$J(\boldsymbol{q})=\sum_{k=1}^{M}\Gamma(M,k)[Y(k)-\boldsymbol{H}^T(k)\hat{\boldsymbol{q}}(k)]^2 \qquad \ldots (12)$$

where, M is the number of data sets used for parameter identification; $\Gamma(M,k)$ is the factor which is constructed as:

$$\Gamma(M,k)=\mu^{M-k}L(k) \qquad \ldots (13)$$

where, μ represents the forgetting factor and satisfies $0<\mu<1$; $L(k)$ means the weighted factor, which is positively defined and well selected according to the different time stamp k.

Remark 2: When the weighted factor $L(k)$ is not considered, the forgetting factor μ makes the weight of the data change with the time stamp, *i.e.*, the weight of the data at k decays by μ compared to $k+1$. When $k=1$, the weight value is minimum and is μ^{M-1}; when $k=M$, the weight value is maximum and is 1. Therefore, the forgetting factor can not only overcome the effect of data saturation, but also suppress the amount of overshoot at the early stage of identification, leading to a smoother parameter identification process.

Remark 3: The weighted factor $L(k)$ is used to obtain the average characteristics of the system and adjust the convergence speed by taking a different value at each time stamp *k*.

Suppose there exists a $\hat{\boldsymbol{q}}$ such that $J(\boldsymbol{q})\big|_{\boldsymbol{q}=\hat{\boldsymbol{q}}}=\min$, then we have:

$$\hat{\boldsymbol{q}}=[\sum_{k=1}^{M}\Gamma(k)\boldsymbol{H}(k)\boldsymbol{H}^T(k)]^{-1}\sum_{k=1}^{M}\Gamma(k)Y(k)\boldsymbol{H}(k) \qquad \ldots (14)$$

The derivation of the FW-RLS algorithm is based on the following steps:

i. Let

$$\bar{\boldsymbol{Q}}(M)=\sum_{k=1}^{M}\Gamma(k)\boldsymbol{H}(k)\boldsymbol{H}^T(k) \qquad \ldots (15)$$

Then, it can be converted as:

$$\bar{\boldsymbol{Q}}(M)=\mu\bar{\boldsymbol{Q}}(M-1)+L(M)\boldsymbol{H}(M)\boldsymbol{H}^T(M) \qquad \ldots (16)$$

ii. From equations (14) and (15), it leads to:

$$\bar{\boldsymbol{Q}}(M)\hat{\boldsymbol{q}}(M)=\bar{\boldsymbol{Q}}(M-1)\hat{\boldsymbol{q}}(M-1)+\Gamma(M)Y(M)\boldsymbol{H}(M) \qquad \ldots (17)$$

iii. Substituting (16) into (17), it is obtained that:

$$\hat{\boldsymbol{q}}(M)=\frac{\hat{\boldsymbol{q}}(M-1)}{\mu}+L(M)[Y(M)-\frac{\boldsymbol{H}^T(M)\hat{\boldsymbol{q}}(M-1)}{\mu}]\bar{\boldsymbol{Q}}^{-1}(M)\boldsymbol{H}(M) \qquad \ldots (18)$$

iv. To avoid the operation of the inverse matrix of $\bar{\boldsymbol{Q}}$, the following variable is constructed:

$$\boldsymbol{P}(M)=\bar{\boldsymbol{Q}}^{-1}(M)=[\mu\boldsymbol{P}^{-1}(M-1)+\Lambda(M)\boldsymbol{H}(M)\boldsymbol{H}^T(M)]^{-1} \qquad \ldots (19)$$

Lemma 1 (Matrix inversion lemma) Let $\boldsymbol{A}\in\Re^{n\times n},\boldsymbol{B}\in\Re^{m\times m},\boldsymbol{C}\in\Re^{n\times m},\boldsymbol{D}\in\Re^{m\times n}$, and the matrices $\boldsymbol{A}$ and $\boldsymbol{B}$ are invertible, then the following equation holds:

$$(\boldsymbol{A}+\boldsymbol{C}\boldsymbol{B}\boldsymbol{D})^{-1}=\boldsymbol{A}^{-1}-\boldsymbol{A}^{-1}\boldsymbol{C}(\boldsymbol{B}^{-1}+\boldsymbol{D}\boldsymbol{A}^{-1}\boldsymbol{C})^{-1}\boldsymbol{D}\boldsymbol{A}^{-1} \qquad \ldots (20)$$

Therefore, (19) can be converted to the following equation:

$$\boldsymbol{P}(M)=\frac{\boldsymbol{P}(M-1)}{\mu}-\frac{\boldsymbol{P}(M-1)\boldsymbol{H}(M)\boldsymbol{H}^T(M)\boldsymbol{P}(M-1)}{\frac{\mu^2}{L(M)}+\mu\boldsymbol{H}^T(M)\boldsymbol{P}(M-1)\boldsymbol{H}(M)} \qquad \ldots (21)$$

v. From equations (18), (19), and (21), the core of the dedicated FW-RLS algorithm is finally expressed as follows:

$$\begin{cases}\hat{\boldsymbol{q}}(M)=\dfrac{\hat{\boldsymbol{q}}(M-1)}{\mu}+L(M)[y(M)-\dfrac{\boldsymbol{H}^T(M)\hat{\boldsymbol{q}}(M-1)}{\mu}]\boldsymbol{P}(M)\boldsymbol{H}(M)\\ \boldsymbol{P}(M)=\dfrac{\boldsymbol{P}(M-1)}{\mu}-\dfrac{\boldsymbol{P}(M-1)\boldsymbol{H}(M)\boldsymbol{H}^T(M)\boldsymbol{P}(M-1)}{\frac{\mu^2}{\Lambda(M)}+\mu\boldsymbol{H}^T(M)\boldsymbol{P}(M-1)\boldsymbol{H}(M)}\end{cases} \qquad \ldots (22)$$

Results and Discussion

In order to verify the performance of the proposed FW-RLS algorithm, the following simulation results will be presented to visualize the superiority of the FW-RLS algorithm.

Modelling and simulation parameters

The following simulation is designed based on the REMUS model, whose modeling data are shown in Table 1. It is worth mentioning that in this simulation, the rudder angle to the right is specified as positive, so the values of $Y_{uu\delta}$ and $N_{uu\delta}$ are taken as -9.64 kg/(m·rad) and 6.15 kg/rad instead of 9.64 kg/(m·rad) and -6.15 kg/rad.

Table 1 — Model parameters of the REMUS marine robot

Parameter	Value	Units
m	29.9	kg
x_G	0	m
u	1.5	m/s
I_z	3.45	kg/m^2
$Y_{\dot{v}}$	-35.5	kg
$Y_{\dot{r}}$	1.93	kg·m/rad
Y_{uv}	-28.6	kg/m
Y_{ur}	5.22	kg/rad
$Y_{uu\delta}$	-9.64	kg/(m·rad)
$N_{\dot{v}}$	1.93	kg·m
$N_{\dot{r}}$	-4.88	kg·m^2/rad
N_{uv}	-24	kg
N_{ur}	-2	kg·m/rad
$N_{uu\delta}$	6.15	kg/rad

To integrate the parameters in the maneuvering model and represent the relationship between rudder angle and yaw angular velocity more intuitively, the REMUS model will be transformed into the equivalent second-order K-T equation as shown in equation (5). With the help of equation (6), its maneuvering equation in horizontal motion can be expressed as:

$$\ddot{r} + 2.2256\dot{r} + 2.9686r = 2.2071\delta + 2.2309\dot{\delta} \quad \ldots (23)$$

The parameters of the FW-RLS algorithm in the simulation are listed in Table 2.

Zigzag maneuvering

This subsection shows the parameter identification results when the rudder is adjusted as a zigzag shape and neglecting the environment disturbance.

In Figure 1, the variation of the yaw angle of REMUS is shown when the rudder is adjusted in 20/20 deg zigzag shape, namely, when the yaw angle exceeds 20° with the help of 20° rudder angle, the rudder angle is changed as -20°, and vice versa.

In addition, to better reflect the performance of the FW-RLS algorithm, the recursive least squares (RLS) method will be used as a benchmark, where the difference between these two algorithms is that the RLS method has no weighted factor and forgetting factor, and $\Gamma(M,k)$ is chosen as 1.

Table 2 — Simulation parameters

Parameter	Value	Units
M	20	s
dt	0.1	s
$\boldsymbol{P}$	10^{10}eye(4)	\
$\boldsymbol{q}(0)$	10^{-10}[1;1;1;1]	\
μ	0.999	\
$L(k)$	20	\

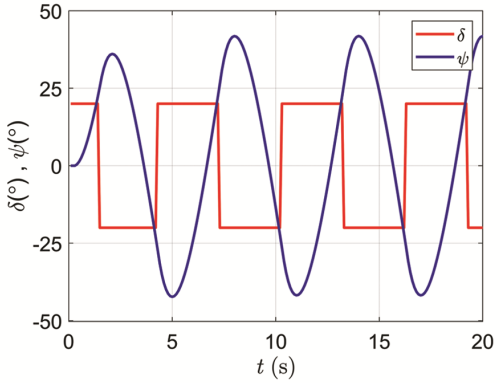

Fig. 1 — Zigzag maneuvering results regarding rudder angle and yaw angle

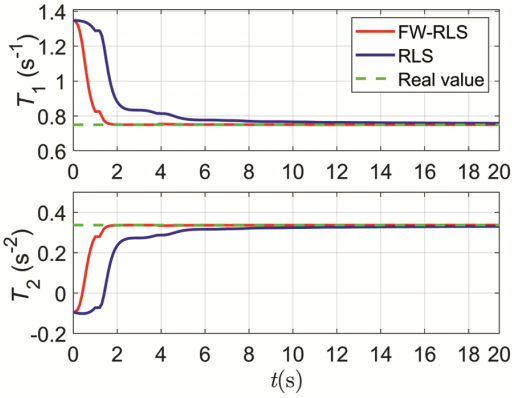

Fig. 2 — Identification results for T_1 and T_2

The results of parameter identification using FW-RLS and RLS are shown in Figures 2 & 3. The figures show that both algorithms can achieve parameter identification for the maneuvering model. However, FW-RLS has a faster convergence rate and a minor overshoot than RLS. Taking T_3 as an example, RLS costs about 4 s to converge and its overshoot is 7.2°, while FW-RLS takes only 1.6 s to converge and its overshoot is only 0.84°. Furthermore, Figures 4 & 5 show the error curves of parameter identification; where $X_e = X_{identification} - X_{real}$, $X = T_1, T_2, K, T_3$. It can be

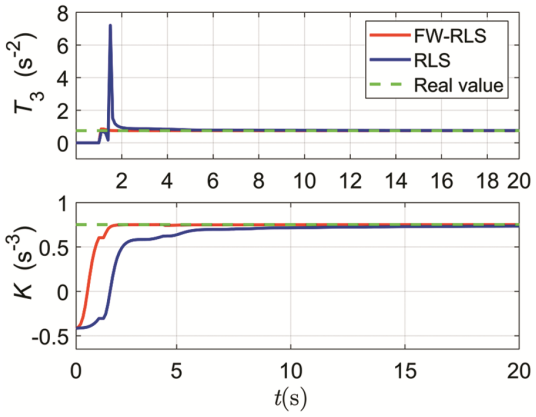

Fig. 3 — Identification results for T_3 and K

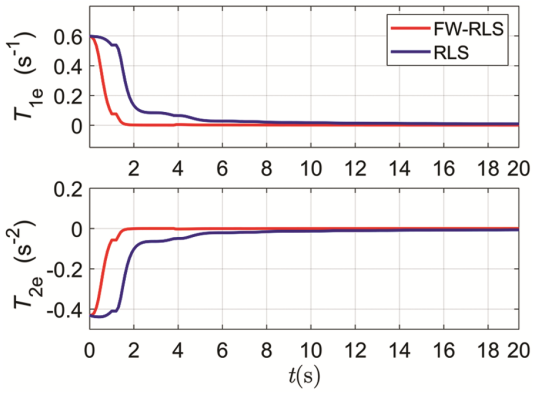

Fig. 4 — Identification errors for T_1 and T_2

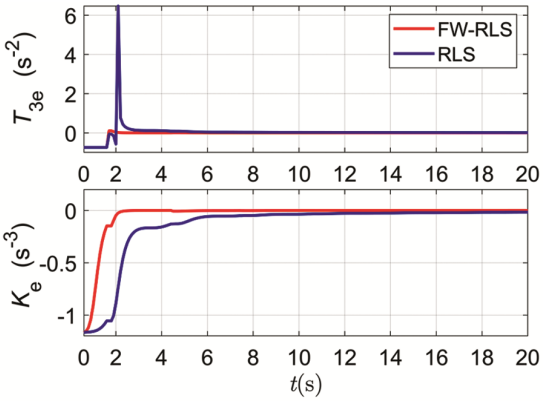

Fig. 5 — Identification errors for T_3 and K

seen that FW-RLS has faster convergence rate and higher identification accuracy than RLS.

Algorithm predictive ability

To verify the predictive ability of the algorithm, the zigzag maneuvering with different rudder angles was used and the corresponding identification data were obtained, as shown in Table 3. Without loss of generality, rudder angles are chosen as 10°, 15° and 20°.

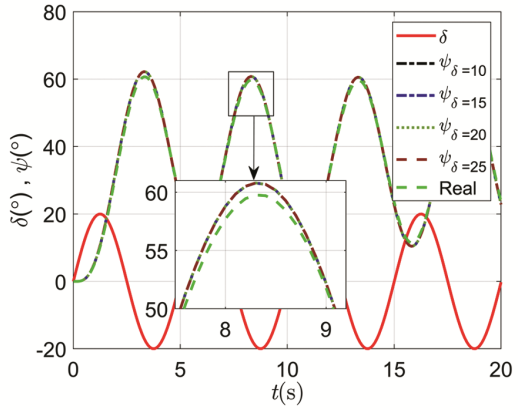

Fig. 6 — Algorithm prediction in sinusoidal shape maneuvering

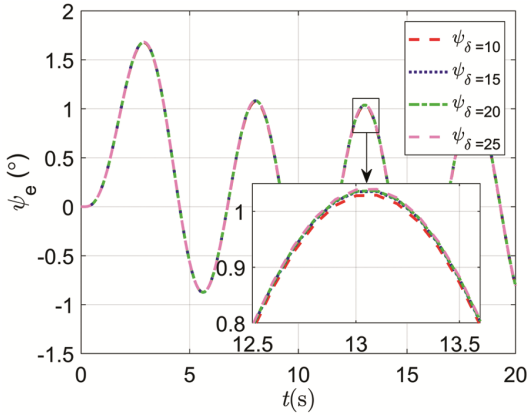

Fig. 7 — Algorithm prediction errors in sinusoidal shape maneuvering

Table 3 — Parameter identification with different maneuvering rudder angles

Parameter	T_1 (s^{-1})	T_2 (s^{-2})	T_3 (s^{-2})	K (s^{-3})
$\delta = 10^\circ$	2.2293	2.9718	2.2112	2.2305
$\delta = 15^\circ$	2.2265	2.9694	2.2082	2.2308
$\delta = 20^\circ$	2.2209	2.9647	2.1020	2.2315
$\delta = 25^\circ$	2.2251	2.9682	2.2066	2.2310
Real Value	**2.2256**	**2.9686**	**2.2071**	**2.2309**

Additionally, the real values in Table 3 are obtained by equation (6). As can be seen from the table, the difference in the parameters obtained from the identification against different rudder angles is within ± 0.01.

Ulteriorly, to visualize the predictive ability of the algorithm, the maneuvering equation is constructed using the identification results obtained by different rudder angles, as shown in Figure 6. It can be visualized from the figure that identification curves showed little difference from the actual curves. Furthermore, Figure 7 shows the error curves of Figure 6, where $\psi_e = \psi_{identification} - \psi_{real}$, and it can be

seen that the errors of the yaw angles from the models with identification parameters are within 2°, which shows that the FW-RLS has the good predictive ability and identification accuracy.

Conclusions

To obtain the parameters of horizontal maneuvering equations of marine robot, FW-RLS is proposed in this paper for parameter identification of the maneuvering equation. Firstly, the second-order K-T equation in horizontal motion, which has only four parameters to be identified, is used as the marine robot's maneuvering equation. Secondly, with the help of the traditional batch least squares method, the FW-RLS algorithm is proposed. Finally, the superiority of the FW-RLS algorithm is verified by numerical simulations. Namely, the convergence rate of the FW-RLS algorithm is twice as much as the RLS algorithm, and the overshoot is about one-tenth of the RLS algorithm. Moreover, FW-RLS has higher identification accuracy and better predictive ability.

Nevertheless, the current algorithm validation is only by numerical simulation, so the algorithm's performance will be further verified in the experiments in the future. In addition, the effect of environmental disturbance is not considered in the horizontal second-order K-T equation, which will degrade the modeling accuracy to some extent, so the subsequent work will take the disturbance into account to further improve the modeling accuracy.

Acknowledgments

This work was supported in part by the National Natural Science Foundation of China under Grant 51909161, in part by the Shanghai Sailing Program under Grant 19YF1424100, in part by the Open Research Fund of Key Laboratory of Marine Environmental Survey Technology and Application, Ministry of Natural Resources under Grant MESTA-2020-B008, in part by the Open Research Fund of State Key Laboratory of Ocean Engineering under Grant 1914, in part by the Key Prospective Research Fund of Shanghai Jiao Tong University under Grant 2020QY10, and in part by the Startup Fund for Youngman Research at SJTU under Grant 19X100040001.

Conflict of Interest

The authors declare that they have no known competing financial interests or personal relationships that could have appeared to influence the work reported in this paper.

Author Contributions

YMZ has contributed in conceptualization, methodology, software, writing - original draft and writing - review & editing. CYY has been engaged in funding acquisition, resources, writing - review & editing, methodology and supervision. CHL has helped in software, visualization and supervision. TML has given a contribution to software, visualization and supervision. RW has helped in methodology and visualization. LL has helped in funding acquisition, resources and supervision.

References

1 Wang Z, Yang S L, Xiang X B, Vasilijevic A, Miskovic N, *et al*., Cloud-based mission control of USV fleet: Architecture, implementation and experiments, *Control Eng Pract*, 106 (2021) p. 104657.

2 Yu C Y, Liu C H, Lian L, Xiang X B & Zeng Z, ELOS-based path following control for underactuated surface vehicles with actuator dynamics, *Ocean Eng*, 187 (2019) p. 106139.

3 Rout R, Cui R X & Han Z Q, Modified line-of-sight guidance law with adaptive neural network control of underactuated marine vehicles with state and input constraints, *IEEE T Contr Syst T*, 28 (2020) 1902-1914.

4 Peng Z H, Liu L & Wang J, Output-feedback flocking control of multiple autonomous surface vehicles based on data-driven adaptive extended state observers, *IEEE T Cybernetics*, 51 (2021) 4611-4622.

5 Wang N & Ahn C K, Hyperbolic-tangent LOS guidance-based finite-time path following of underactuated marine vehicles, *IEEE T Ind Electron*, 67 (2019) 8566-8575.

6 Liu X, Zhang M J, Wang Y J & Rogers E, Design and experimental validation of an adaptive sliding mode observer-based fault-tolerant control for underwater vehicles, *IEEE T Contr Syst T*, 27 (2019) 2655-2662.

7 Gao J, Liang X M, Chen Y M, Zhang L J & Jia S S, Hierarchical image-based visual serving of underwater vehicle manipulator systems based on model predictive control and active disturbance rejection control, *Ocean Eng*, 229 (2021) p. 108814.

8 Mei J H & Arshad M R, A smart navigation and collision avoidance approach for autonomous surface vehicle, *Ind J Geo-Mar Sci*, 46 (2017) 2415-2421.

9 Xiang G & Xiang X B, 3D trajectory optimization of the slender body freely falling through water using cuckoo search algorithm, *Ocean Eng*, 235 (2021) p. 109354.

10 Zheng Z W, Moving path following control for a surface vessel with error constraint, *Automatica*, 118 (2020) p. 109040.

11 Wu B J, Han X W & Hui N M, System identification and controller design of a novel autonomous underwater vehicle, *Machines*, 9 (2021) p. 109.

12 Yang Y, Pang Y J, Li H W & Zhang R B, Local path planning method of the self-propelled model based on reinforcement learning in complex conditions, *J Mar Sci Appl*, 13 (2014) 333-339.

13 Xia L, Yuan S, Zou Z J & Zou L, Uncertainty quantification of hydrodynamic forces on the DTC model in shallow water

waves using CFD and non-intrusive polynomial chaos method, *Ocean Eng*, 198 (2020) p. 106920.

14 Hou X R, Zou Z J & Liu C, Nonparametric identification of nonlinear ship roll motion by using the motion response in irregular waves, *Appl Ocean Res*, 73 (2018) 88-99.

15 Dong Z P, Yang X, Zheng M, Song L F & Mao Y S, Parameter identification of unmanned marine vehicle manoeuvring model based on extended Kalman filter and support vector machine, *Int J Adv Robot Syst*, 16 (2019) 2509-2519.

16 Wang Z H, Zou Z J & Guedes S C, Identification of ship manoeuvring motion based on nu-support vector machine, *Ocean Eng*, 183 (2019) 270-281.

17 Wang Z H, Xu H T, Xia L, Zou Z J & Guedes S C, Kernel-based support vector regression for nonparametric modeling of ship maneuvering motion, *Ocean Eng*, 216 (2019) p. 107994.

18 Xu H T, Hassani V & Guedes S C, Comparing generic and vectorial nonlinear manoeuvring models and parameter estimation using optimal truncated least square support vector machine, *Appl Ocean Res*, 97 (2020) p. 102061.

19 Zhang G, Zhang X & Pang H, Multi-innovation auto-constructed least squares identification for 4 DOF ship manoeuvring modelling with full-scale trial data, *ISA T*, 58 (2015) 186-195.

20 Wang H, Zheng Y P & Yu Y, Lithium-ion battery SOC estimation based on adaptive forgetting factor least squares online identification and unscented kalman filter, *Mathematics-basel*, 9 (2020) p. 1733.

21 Xu K, Yang J, Fan W W, Tang C S & Li T, Forgetting factor least square parameter identification based on tool servo speed tracking of the milling process, *J Eng Sci Tech Rev*, 13 (2020) 22-29.

22 Liu S Q, Wang J H & Fang Z J, Improved FEM for distribution network cables rating using multiple forgetting factors least-square, *AIP Adv*, 8 (2018) p. 105030.

23 Geng P B, Wang J & Chen W G, Multipath least squares algorithm and analysis, *Signal Process*, 174 (2020) p. 107633.

24 Cohen A & Migliorati G, Optimal weighted least-squares methods, *J Comput Math*, 3 (2016) 181-203.

25 Mohamadipanah H, Heydari M & Chowdhary G, Deep kernel recursive least-squares algorithm, *Nonlinear Dynam*, 104 (2021) 2515-2530.

26 Ren B Y, Xie X, Sun X D, Zhang Q & Yan D, Parameters identification of lithium-ion battery based on the improved forgetting factor recursive least squares algorithm, *IET Power Electron*, 13 (2020) 2531-2537.

27 Prestero T, *Verification of a six-degree of freedom simulation model for the REMUS autonomous underwater vehicle*, Master thesis, Massachusetts Institute of Technology, 2001.